
# Grasping with a new hand

Valyear, Kenneth F.; Mattos, Daniela; Philip, Benjamin A.; Kaufman, Christina; Frey, Scott H.

**Neuroimage**

*DOI:*
10.1016/j.neuroimage.2017.09.052

Published: 15/04/2019

Peer reviewed version

# Grasping with a new hand: Improved performance and normalized grasp-selective brain responses despite persistent functional changes in primary motor cortex and low-level sensory and motor impairments.

Kenneth F. Valyear[1, 2], Daniela Mattos[2], Benjamin A. Philip[2], Christina Kaufman[3], and Scott H. Frey[2].

[1]School of Psychology, Bangor University, Bangor, UK.
[2]Department of Psychological Sciences, University of Missouri, Columbia, MO.
[3]Christine M. Kleinert Institute, Louisville, KY.

For submission to the journal *NeuroImage*

**Abbreviated Title: Grasping with a new hand**

*Correspondence should be addressed to:*

Ken Valyear, Ph.D.
Bangor University
School of Psychology
Brigantia Building
Bangor, UK LL57 2AS
Email: k.valyear@bangor.ac.uk

*Or*

Scott H. Frey, Ph.D.
University of Missouri
Department of Psychological Sciences
McAlester Hall
Columbia, MO 65211
Email: freys@missouri.edu
Phone: 573-818-4020

Conflict of Interest: No conflicts of interest.

**Acknowledgements:** This work was supported by research grants from the Department of Defense (W81XWH-13-1-0496) and the National Institutes of Health (NS083377) to Scott H. Frey.

**ABSTRACT**

Hand loss can now be reversed through surgical transplantation years or decades after amputation. Remarkably, these patients come to use their new hand to skilfully grasp and manipulate objects. The brain mechanisms that make this possible are unknown. Here we test the hypothesis that the anterior intraparietal cortex (aIPC) – a multimodal region implicated in hand preshaping and error correction during grasping – plays a key role in this compensatory grasp control. Motion capture and fMRI are used to characterize hand kinematics and brain responses during visually guided grasping with a transplanted hand at 26 and 41 months post-transplant in patient DR, a former hand amputee of 13 years. Compared with matched controls, DR shows increasingly normal grasp kinematics paralleled by increasingly robust grasp-selective fMRI responses within the very same brain areas that show grasp-selectivity in controls, including the aIPC, premotor and cerebellar cortices. Paradoxically, over this same time DR exhibits significant limitations in basic sensory and motor functions, and persistent amputation-related functional reorganization of primary motor cortex. Movements of the non-transplanted hand positively activate the ipsilateral primary motor hand area – a functional marker of persistent interhemispheric amputation-related reorganization. Our data demonstrate for the first time that even after more than a decade of living as an amputee the normative functional brain organization governing the control of grasping can be restored. We propose that the aIPC and interconnected premotor and cerebellar cortices enable grasp normalization by compensating for the functional impact of reorganizational changes in primary sensorimotor cortex and targeting errors in regenerating peripheral nerves.

## INTRODUCTION

Upper extremity amputation causes major disability and adversely impacts body image (Gaine et al., 1997), and the rates of rejection for prosthetic devices are high (Biddiss et al., 2007). Allogeneic hand transplantation offers an alternative intervention, and the number of individuals having undergone this procedure now exceeds 75 (Shores et al., 2015). Despite persistent and significant limitations in basic sensory and motor functions (Breidenbach et al., 2008; Landin et al., 2012), kinematic measures of reach-to-grasp reveal remarkably proficient use of the grafted hand to grasp and manipulate objects (Huchon et al., 2016). The brain mechanisms that enable this recovered functional use of the hand are unknown, and are the focus of this study.

Both animal model and human data converge on the fact that injuries to the peripheral nerves, including upper extremity amputation, lead to “massive” changes in the functional organization of the undamaged motor and sensory cortices (Pons et al., 1991; Ramachandran et al., 1992). As a result of decreased afferent/efferent activity, there is an expansion of adjacent maps into the cortical territory formerly devoted to the affected body part (Merzenich et al., 1984; Garraghty and Kaas, 1991). For hand amputees, such plasticity has been demonstrated in representations of the laterally neighboring face (Elbert et al., 1994; Yang et al., 1994; Flor et al., 1995; Karl et al., 2001), medially adjacent residual limb (Cohen et al., 1991a; Lotze et al., 2001), and even interhemispherically, as seen for movements of the intact hand (Hamzei et al., 2001; Bogdanov et al., 2012).

The functional significance of these changes is controversial, and a topic of ongoing interest (Flor et al., 1995; Frey et al., 2008; Flor et al., 2013; Makin et al., 2013; Frey, 2014; Philip and Frey, 2014; Makin et al., 2015). It has, however, been suggested that persistent reorganization in primary sensorimotor cortex may contribute to poor functional outcomes in human adults following surgical repairs of peripheral nerves in the hand or forearm (Almquist and Eeg-Olofsson, 1970; Wall et al., 1986; Lundborg and Rosen, 2007).

Functional MRI (fMRI) responses during passive sensory stimulation (Neugroschl et al., 2005; Frey et al., 2008; Hernandez-Castillo et al., 2016) or simple volitional movements (Giraux et al., 2001; Lanzetta et al., 2004; Brenneis et al., 2005) of a transplanted hand consistently reveal sustained amputation-related reorganizational changes in primary sensory (S1) and motor (M1) cortices even long after the procedure. These changes, coupled with reinnervation errors in regenerating peripheral nerves, are thought to limit recovery of basic sensory and motor functions (Frey, 2014).

It is well understood that reach-to-grasp movements involve a network of cortical and subcortical structures within the distributed sensorimotor system. Grasping requires configuring the hand according to target object properties (Jeannerod et al., 1995; Castiello, 2005; Grafton, 2010), and even in healthy individuals this necessitates rapid detection and compensation for errors that arise from many sources (Tunik et al., 2005; Rice et al., 2006). An abundance of evidence implicates the aIPC as essential for this adaptive, multimodal control of the hand during visually guided grasp (Binkofski et al., 1998; Culham et al., 2003; Frey et al., 2005). Patients with damage to the aIPC show impaired anticipatory preshaping of the hand during grasping (Binkofski et al., 1998), and perturbing the functions of the aIPC with transcranial magnetic stimulation (TMS) impairs preshaping in healthy controls (Rice et al., 2006; Davare et al., 2007).

On the basis of this evidence, we hypothesize that the aIPC enables successful grasping with a transplanted hand by compensating for errors that arise from limited recovery of basic sensory and motor abilities. Specifically, improvements in hand preshaping during visually guided grasping are predicted to parallel increasingly normative grasp-selective responses in the aIPC, despite persistent basic sensory and motor deficits and S1/M1 reorganizational changes. Functional MRI and high-resolution kinematic recordings are used to evaluate these predictions in DR, a right-hand dominant male who suffered traumatic amputation of his left hand in 1998 (age 23) and underwent hand transplantation 13 years later (age 36). Both

fMRI and behavioral grasping data are collected at 26 (Test 1) and 41 (Test 2) months post-transplant. Functional mapping of primary sensorimotor cortex is completed at 44 months post-transplant. Data are compared with those of healthy controls matched for age, gender and hand dominance.

## MATERIALS AND METHODS

### Hand transplant recipient

DR suffered traumatic transpalmar amputation of his left, non-dominant hand, and a crush injury to his right hand, in 1998 (age 23). He underwent simultaneous surgical amputation of the residual left hand and wrist and left-hand transplantation at the level of the distal forearm 13 years later (age 36). Rejection is controlled with daily oral Prograf and Rapamune. DR has no history of prosthesis use.

### Healthy controls

All controls were male and right-handed, as determined by the Edinburgh handedness questionnaire (Oldfield, 1971), with no prior history of neurological disease. A group of 24 control participants (mean age = 43 yrs., range = 26 - 64 yrs.) took part in the fMRI grasp study. From this group, 17 participants completed the fMRI sensorimotor mapping study (mean age = 45 yrs., range = 27 - 64 yrs.). A separate group of six control subjects (mean age = 33 yrs., range = 27 - 45 yrs.) completed the reach-to-grasp experiment performed outside of the MRI scanner.

All participants provided informed consent in accordance with the University of Missouri IRB and Department of Defense Human Research Protection Office, and received financial compensation for their efforts.

### Behavioral grasping task

Participants sat at a table and performed a reach-to-grasp task. Kinematics were recorded at 100 Hz using an Optotrak Certus (Northern Digital; Toronto, CA) system. Infrared emitters (IRED) were affixed to four locations: (1) the tip of the participant's thumb, (2) the tip of their index finger (3) the middle

phalange of the index finger, and (4) the metacarpophalangeal joint of the index finger. An IRED comprised two adjacent emitters (1-3mm separation).

On each trial, participants were asked to reach-to-grasp an object and place it in a bowl. The objects were small ($1cm^3$), medium ($2cm^3$), and large ($4cm^3$) wooden cubes. Objects were positioned on a flat tray, at a distance that allowed a comfortable reach at less than full arm extension. Between trials, participants kept their hands on a rest key, with their thumbs and index fingers lightly pinched together. The distance between the rest key and the target object, and between the object and the bowl was 20cm. During the inter-trial interval, vision was blocked using Plato visual occlusion spectacles (Translucent Technologies; Toronto, Canada) as the experimenter prepared the next object for the upcoming trial. At the start of each trial, the spectacles cleared allowing the participant to see the object and initiate their reach-to-grasp response. After picking up the object, participants placed the object in a bowl located in front of the body midline, at the same distance as the tray. The spectacles remained clear until participants returned to the start position.

The experiment comprised 96 trials, divided into four blocks of 24 trials each. Each block involved the use of one hand and included 8 repetitions of each of the three object sizes. The same hand was always used for two consecutive blocks. The full experiment included performing movements with both the left and right hands and with and without full vision of the hand. These conditions were run in separate blocks. Only data from the left hand full vision condition is presented here (24 trials), for purposes of comparison with the fMRI task. Object size was counterbalanced within each block. Hand and visual condition were counterbalanced across participants.

**Kinematic Data Analysis**

The position of the IREDs was exported to text files using NDI First Principles Motion Capture Software (Northern Digital Inc., Ontario, Canada). The signals were then processed with a customized Matlab program (Mathworks, version R2015b, Massachussets, USA). The data were prepared in three steps: first, marker coordinates were low-pass filtered at 5 Hz with a bidirectional 4th-

order Butterworth filter. Second, trials that had blocked markers during the movement were excluded from the analyses (12.5 % of the trials, 24/192). Next, the mean distances between the two adjacent markers were computed. The time profile of both the grip aperture and the hand transport velocity were then estimated, and time-normalized. The grip aperture was computed as the Euclidean distance between the *x*, *y*, and *z*, coordinates of the index finger and thumb markers.

The resultant velocity of hand transport was obtained after differentiation of the *x*, *y*, *z* coordinates of the metacarpophalangeal joint of the index finger. Movement offset was determined semi-automatically as the time when the velocity profile fell and remained below 5% of its peak for 50ms. This criterion was chosen to isolate the reach-to-grasp phase – the remaining parts of trials were not analyzed. Movement time (MT) was calculated as the time between movement onset (at the button release) and offset. The following kinematic variables were defined: peak grip aperture (pGA); time to peak grip aperture (ttpGA); peak transport velocity (pV); time to peak transport velocity (ttpV). The temporal variables are reported in percentage of the movement time. For the control group, descriptive statistics were reported (including means, standard deviations, and 95% confidence intervals).

**fMRI grasping task**

Participants manually interacted with a plastic cube ($2cm^3$) presented using the apparatus shown in **Figure 1**. The platform was specifically adjusted for each individual so that the cube could be reached with minimal movement of the arm, and the workspace could be viewed through mirrors. The problems associated with movements of the head were thoroughly explained, and participants were told that their hand actions should not involve movements of the upper arm or shoulder, and that their head should be kept still at all times. Padding was used to elevate the arms, and an adjustable strap was fastened across the upper arms and chest to further minimize potential shoulder movements (not shown in Fig 1A).

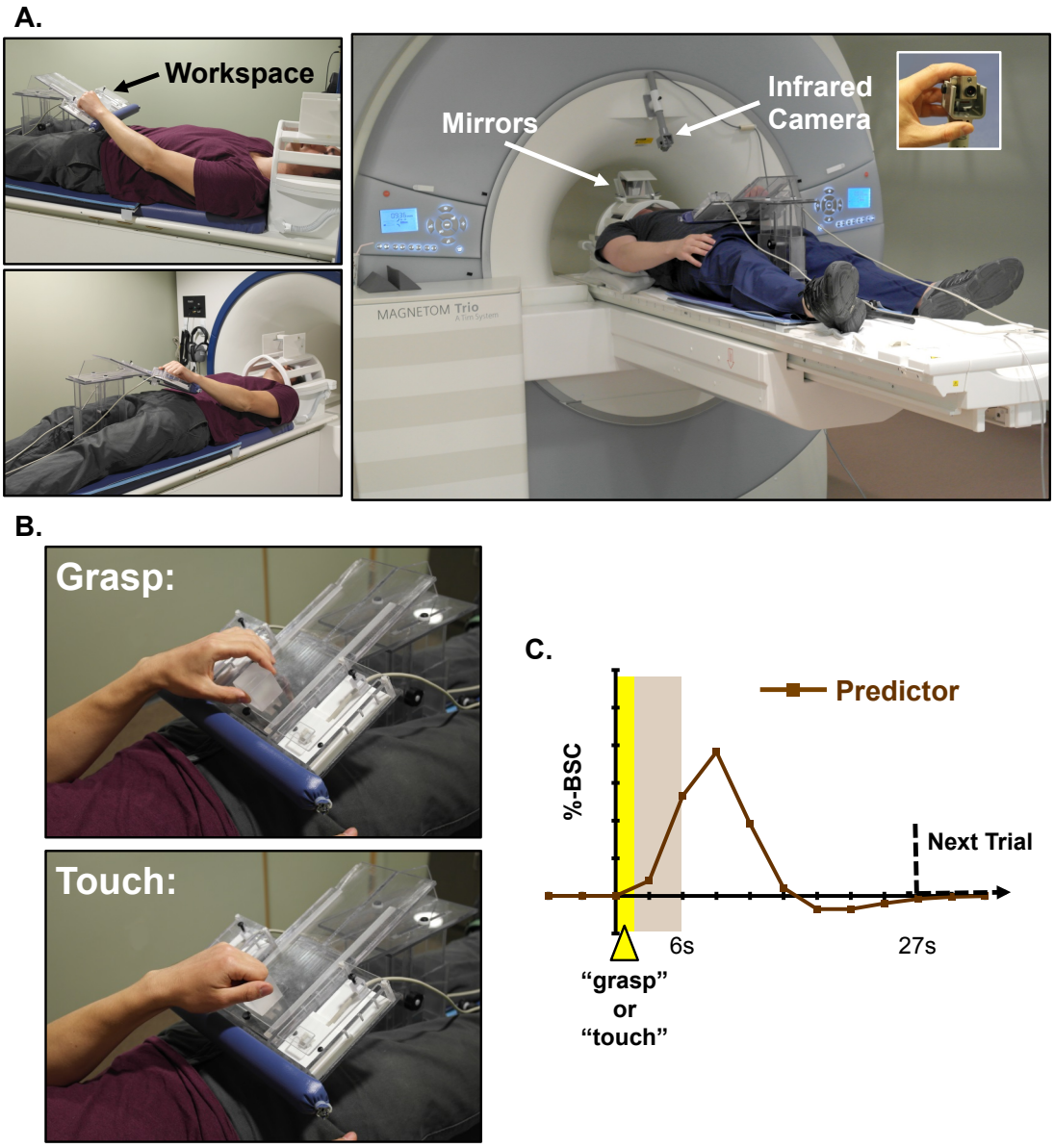


**Fig 1. Methods.** (A) Setup showing the apparatus used to present the target object. (B) Experimental conditions involved Grasp or Touch actions. (C) Timing of events within and between trials, and the shape and timing of the predictor function used in the general linear model.

In the start position, participants rested the hand they were instructed to use for grasping (the left hand) in a relaxed posture (visible in the top left photographs, Fig 1A). The distance from the resting hand position to the target cube was ~11cm, on-center. Their other hand was positioned along their side and remained still. Participants were instructed to close their eyes during rest periods, and to listen for auditory cues: "grasp" or "touch". When they heard "grasp", they opened their eyes, transported the left hand to the target and gripped the cube along its y-dimension, using a lateral pinch with

their thumb and fingers in opposition. They then returned to the rest position, closed their eyes and awaited the start of the next trial. They were instructed to move slowly and smoothly, and to lightly grip the cube. Similarly, when they heard “touch”, they opened their eyes and touched the cube near its center using the proximal interphalangeal joints of the hand, and then returned to the start position. An MR-compatible camera system (MRC Systems GmbH) was used to record participants’ hand actions; videos were evaluated offline for errors.

Grasp and touch conditions were defined as 6s periods, beginning with (500ms duration) auditory cues, followed by 21s rest periods to allow for the blood oxygen-level dependent (BOLD) signal to return to baseline levels. Each run began with 12s of rest, comprised 16 trials (8 per condition), and lasted 7min and 33s. Participants performed five runs. A custom Matlab (R2011b) script was used to create 6 distinct run orders whereby trial history (N-1) was balanced for condition within runs. Run orders were randomized for presentation across individuals (although N = 6 controls received orders 1-5, in that sequence).

Absent or incorrect responses were excluded from analyses (i.e., assigned a predictor of no interest in the GLM). Due to technical problems, 5% (95/1920 trials) of video data from controls were unavailable. Specifically, in four subjects one complete run was unavailable, while in four other subjects, 2, 2, 8, and 9 trials of video data were not collected.

Video data confirm that DR performed the task correctly in 77/80 trials during Test 1. He did not respond during two trials of one run, and responded incorrectly (performing a Touch instead of a Grasp response) during one trial of a separate run. During Test 2, DR correctly responded in 70/80 trials; he reported falling asleep during part of two runs and hence did not respond for 9/32 of these trials. He also responded incorrectly (performing a Grasp instead of a Touch response) during one trial in a separate run.

Control participants performed correctly in 1801/1825 trials (mean = 1 +/- 1.9). Errors included no responses (mean = 0.13 +/- 0.49), prolonged holding of object after grasping (mean = 0.13 +/- 0.49), multiple grasps during the same trial (mean = 0.08 +/- 0.28), and incorrect responses (mean = 0.67 +/- 1.7) (total errors = 3, 3, 2, and 16, respectively).

**fMRI sensorimotor mapping task**

Participants were positioned supine in the scanner and moved different body parts according to auditory cues: “left hand”, “right hand”, “left foot”, “right foot”, or “lips”. Each cue was followed by a series of 10 tones presented at a rate of 1 Hz, and participants were instructed to move the cued body part in pace with the onset of each tone. Movement blocks ended with the cue “stop”, and were 13s in duration including movement instruction and stop cues. Each movement block was followed by 18s rest-periods. Participants were asked to keep their eyes closed throughout.

Movements of the hands and feet involved small-amplitude flexion-extension movements of the fingertips and toes, respectively. Mouth movements involved pursing the lips while keeping the jaw and mouth closed and motionless. Prior to scanning, the experimenter demonstrated appropriate movements for each condition. The importance of keeping the head still was emphasized.

Each run began with 8s of rest, comprised 10 movement condition blocks (two per condition), and lasted 5min and 18s. A custom Matlab (R2011b) script was used to create four distinct run orders whereby block history (N-1) was balanced for condition within runs. Participants completed four runs, each with a distinct condition-presentation order.

**Imaging parameters**

Imaging was performed on a 3-Tesla Siemens TIM Trio MRI scanner with a conventional 8-channel birdcage head coil. The T1-weighted anatomical images were collected using a multiplanar rapidly acquired gradient echo (MP-RAGE) pulse sequence: time to repetition (TR) = 1920ms; time to echo

(TE) = 2.92ms; flip angle = 9°; matrix size = 256 x 256; field of view (FOV) = 256mm; 176 contiguous sagittal slices; slice thickness = 1mm; in-plane resolution = 1mm x 1mm. Auto Align Scout and True FISP sequences were executed before the start of each functional run to ensure that slices were prescribed in exactly the same positions across runs. Functional MRI volumes were collected using a T2*-weighted single-shot gradient-echo echo-planar imaging (EPI) acquisition sequence: TR = 3000ms; TE = 30ms; flip angle = 84°; matrix size = 64 x 64; FOV = 200mm; slice thickness = 3mm; in-plane resolution = 3.125mm x 3.125mm; acceleration factor (integrated parallel acquisition technologies, iPAT) = 2 with generalized auto-calibrating partially parallel acquisitions (GRAPPA) reconstruction. Each volume comprises 48 contiguous (no gap) axial slices spanning from the most superior point of cortex ventrally to include the entire cerebellum (i.e. whole-brain coverage).

**fMRI data preprocessing and analyses**

Imaging data were preprocessed and analyzed using tools from fMRIB Software Library (FSL v.5.0.4; http://fsl.fmrib.ox.ac.uk/fsl) (Smith et al., 2004). Each functional run was assessed for subject head motion by first examining cineloop animations and then motion-detection parameter plots generated by FSL 3-D motion correction algorithms on the untransformed two-dimensional data. Non-brain structures were removed using BET.

Functional data were preprocessed with high-pass temporal frequency filtering to remove frequencies below 0.01 Hz. Functional volumes were then aligned to high-resolution anatomical volumes using FLIRT, and transformed to standard stereotaxic space (Montreal Neurological Institute, MNI-152 template) using FNIRT nonlinear registration algorithims. Data were spatially smoothed using a Gaussian kernel of 6mm (full-width at half-maximum).

Data were analyzed at single-subject levels using fixed-effects general linear models (GLMs), carried out in FEAT v.6.0, with FILM applied to correct for serial correlations (Woolrich et al., 2001). To enable valid between-run and -subject statistics, each run underwent intensity normalization using “grand mean scaling”, effectively giving each run a mean signal of zero and

converting beta weights to units of standard deviations. Group-level voxel-wise analyses were implemented using random-effects, FLAME 1 (Woolrich et al., 2004). The Duvernoy anatomical atlas was used as a guide to name active brain areas (Duvernoy, 1999).

GLMs included independent explanatory variables (EVs) per condition, and their temporal derivatives. Condition-specific EVs were modeled as rectangular wave functions, high during the condition and low during all other conditions, convolved with a double-gamma basis function to estimate spatiotemporal properties of the BOLD response, aligned to the onset of auditory cues (**Fig 1C**). For runs without Errors, "dummy" predictors comprising columns of all zeros in the design matrix were included. Additional EVs of non-interest included head motion translation/rotation parameters from motion correction outputs, and spike predictors corresponding to abrupt signal changes between temporally adjacent volumes of +/- 1 SD from the mean, as identified using FSL outlier detection.

**fMRI grasping task**

***Voxel-wise analyses***

Per individual, four orthogonal contrasts (one-tailed t tests) were carried out at the first-level, single-run analyses: (1) Grasp > rest; (2) Touch > rest; (3) Grasp > Touch; (4) Touch > Grasp. The resulting contrasts of parameter estimates (COPEs) then served as input to higher-level, across-run (second level), fixed-effects analyses, and for controls, across subject (third level), random-effects analyses. Unless otherwise indicated, Z-statistical maps were thresholded at Z = 2.3, $p < 0.011$, cluster-size corrected for multiple comparisons at $p < 0.05$. The contrast Grasp > Touch was used to identify areas exhibiting grasp-selective responses.

***Functional-anatomical masks***

At both the individual-subject and group levels, final GLM results were constrained according to functionally- and anatomically-defined inclusive masks. The purpose of this method was to increase the sensitivity of subsequent statistical tests (i.e. Grasp > Touch) by reducing the number of

voxels considered for correction for multiple comparisons to those that (1) showed task-related activity increases (functional criterion) and (2) were likely to overlap with brain areas important for sensorimotor control of the hand (anatomical criterion). This was particularly useful given our aim to characterize grasp-related activity at individual-subject/patient levels, where, due to limited data, the use of corrected thresholds may be too conservative (Smith et al., 2005; Lieberman and Cunningham, 2009).

Functional masks were defined at single-subject (second level, fixed effects) and group (third level, random effects) levels by selecting those voxels significantly active for either (1) Grasp > rest, or (2) Touch > rest, thresholded at $Z = 3.1$, $p < 0.001$, uncorrected.

The following anatomical masks were defined according to the Juelich Histological Atlas (JHA), Harvard-Oxford Subcortical Atlas (HOSA), or the Cerebellar Atlas in MNI-152 space after normalization with FNIRT (CerebA-152). All structures were defined bilaterally at a minimum subject-overlap threshold of > 5%.

- Structures defined by the JHA: (1) Anterior Intraparietal Sulcus (hIP1, hIP2, hIP3); (2) Primary Motor Cortex (BA4a, BA4p); (3) Primary Somatosensory Cortex (BA1, BA2, BA3a, BA3b); (4) Secondary Somatosensory Cortex/Parietal Operculum (OP1, OP2, OP3, OP4); (5) Premotor Cortex (BA6); (6) Ventral Premotor Cortex/Broca's Area (BA44).
- Structures defined by the HOSA: (1) Pallidum; (2) Putamen; (3) Caudate; (4) Thalamus.
- Structures defined by the CerebA-152: (1) Cerebellum (bilateral lobules and the Vermis: IV; V; VI; Crus I; Crus II; VIIb; VIIIa; VIIIb; IX; X).

Functional-anatomical masks were defined by conjoining those voxels that satisfied both functional and anatomical criterion. In other words, the resultant masks comprised voxels within the specified anatomical structures that were also significant activated above rest for either Grasp or Touch conditions.

***Voxel-wise single-subject-overlap maps***

A critical aim was to characterize the patterns of activity associated with grasping at the single-subject/patient levels. To summarize these results in our group of healthy controls, we created a statistical map that reflects the number of overlapping subjects per voxel showing significant Grasp > Touch activity as qualified at single-subject thresholds. The approach provides a reasonable estimate of the probable range of variable grasp-selective responses in healthy controls at single-subject-levels. Critically, because thresholds were the same for all controls and DR (set to a minimum Z = 2.3, $p < 0.011$, cluster-size corrected for multiple comparisons at $p < 0.05$), this approach permits direct comparison of controls' data with those of patient DR from either testing session.

To quantify these data, we calculated the proportion of active voxels in DR at Tests 1 and 2 that are non-overlapping with at least one control participant's thresholded activity map. We then used the same approach to estimate the probable range of uniquely active voxels at individual subject levels in our control group. For each control participant's thresholded maps we calculated the proportion of voxels non-overlapping with at least one other control participant's thresholded map. We then computed the group mean and 95% confidence intervals.

***ROI analyses***

Regions of interest (ROIs) were functionally defined at the group-level in healthy controls based on results of the contrast Grasp > Touch. ROIs included those independent clusters of activity that were: (1) identified at Z = 2.3, $p < 0.011$, uncorrected thresholds, and (2) whereby a minimum of five controls (> 20%) also showed activity in these brain areas at cluster-size corrected thresholds in single-subject analyses.

For each ROI, the voxel with the highest Z-value was identified, a 5mm-diameter-sphere was centered on this coordinate, and all significantly active voxels (thresholded at $p < 0.05$, uncorrected for multiple comparisons) within the sphere were included in computing average percent BOLD signal change

(%-BSC) values from the region. The choice of a more liberal ($p < 0.05$) voxel-selection-threshold was made to increase the chance of equating the sizes of ROIs across brain areas.

Importantly, the data used to define ROIs (from controls) were independent from the data that were extracted and further examined (from patient DR). Extracted data from DR comprised second-level COPEs, expressed as the mean %-BSC values for the contrast Grasp > Touch. To obtain a measure of variability of the COPEs extracted from each ROI we calculated one-sided (lower-bound) 95% confidence intervals around the means according to the standard error measures across runs, using a one-tailed t-statistic with the number of runs as the degrees of freedom.

Although conservative, this was a reasonable approach to evaluate whether DR's fMRI responses within the control-group-defined ROIs reliably showed the predicted Grasp > Touch effects. The alternative, more common method of using the control's data to estimate confidence intervals for comparison is statistically invalid in this case (Kriegeskorte et al., 2009), since the ROIs are defined by the contrast Grasp > Touch. Estimates of effect-sizes and confidence intervals with this approach are biased in the direction of Grasp > Touch; specifically, %-BSC effect sizes would be overestimated and error underestimated.

At the request of an anonymous reviewer, we also performed a leave-one-subject-out (LOSO) analysis (Esterman et al., 2010) to estimate the %-BSC effects sizes and 95% CIs from the control group's data, per ROI. This method is thought to sidestep the problem of non-independence, described above. Group-level GLMs are computed using all but one participant's data. Each new LOSO GLM result is then used to redefine ROIs within the neighborhood of those defined by the full group's model. Specifically, for each LOSO GLM result, we identified the peak Z-value that represents the ROIs defined in the full model, used to evaluate DR's data. A 5mm-diameter-sphere was centered on this coordinate, and those voxels within the sphere that also showed significant Grasp > Touch activity (at $p < 0.05$, uncorrected) for that

particular LOSO GLM result were defined. This method matches precisely the method we used to define ROIs in the full group model, to evaluate DR's data. Critically, for each LOSO GLM result the data from the subject that was left out of the model is extracted per ROI, expressed as %-BSC values for the contrast Grasp > Touch. As such, these data are independent from the data used to define the ROIs. The procedure was repeated, iteratively, until all (24) LOSO GLMs were computed, and for each new ROI, the data from the excluded subject was extracted. The group-level means and 95% CIs were then computed from ROIs that constitute the same brain region (e.g. 24 LOSO-defined ROIs from contralateral primary sensorimotor cortex).

**fMRI sensorimotor mapping task**

***ROI analyses***

The right-hemisphere primary sensorimotor hand area was defined in DR and a subgroup (N=17) of our healthy controls (at single-subject-levels) using the contrast: Left Hand (move) > rest. In each individual, the voxel with the highest Z-value that was also located within primary motor/sensory cortex (25% likelihood of overlapping BA1-4) was identified. All significantly active voxels (thresholded at $Z = 2.3$, cluster-size corrected for multiple comparisons, $p < 0.05$) within a sphere 5mm-diameter-sphere around this coordinate were included.

For each individual for each ROI we then extracted the mean second-level COPEs expressed as the mean %-BSC values for the contrasts: Right Hand > rest, Left Foot > rest, Right Foot > rest, Mouth > rest. For controls, 95% confidence intervals were calculated according to the variability of the mean COPE values across participants.

**RESULTS**

DR exhibits persistent limitations in basic sensory and motor functions and remains dependent on vision when grasping small objects. As summarized in **Table 1**, sensory thresholds are elevated to levels indicative of diminished light touch, and the inability to localize supra-threshold stimuli and to pick up

and identify small objects without vision reflects limited protective sensation. DR is able to experience hot, cold and painful sensations, but remains unable to complete the Grating Orientation (Johnson and Phillips, 1981) and Purdue Pegboard tests (Tiffin and Asher, 1948). His grip strength exhibits some improvements during this same period, but still remains far below that of his natural hand, and he reports a 20% increase in the use of his new hand during unilateral or bilateral activities of daily living. This subjective account is supported by small improvements on tests of hand function performed with vision, including both the Carroll (Carroll, 1965) and Moberg Pickup Tests (Amirjani et al., 2007). However, DR's ability to use his transplanted hand to grasp objects remains highly dependent on vision, making completion of the Moberg Pickup Test impossible with eyes closed.

**Table 1**. *DR's basic-level sensory and motor abilities.*

| | Two Years Post-Transplant | | Four Years Post-Transplant | |
|---|---|---|---|---|
| | **Left Hand** | **Right Hand/Normative** | **Left Hand** | **Right Hand/Normative** |
| **2-point Static**[1] | 15mm | < 6mm | 15mm | < 6mm |
| **2-point Moving**[1] | 14-15mm | 2 - 3mm | 15mm | 2 - 3mm |
| **Semmes-Weinstein Thresholds**[2] | 4.56 | <=2.83 | 4.56 | <=2.83 |
| **Touch Localization w/o vision**[3] | 34.4mm | 6.25mm | 19.1mm | 5.4mm |
| **Grip Force Power Grip** | 21.2lbs | 65.6lbs | 31.6lbs | 77.4lbs |
| **Grip Force Lateral Pinch** | 3.0lbs | N/A | 4.0lbs | N/A |
| **Moberg Test w/ Vision** | 14.6secs | 8.1secs | 12.4secs | 9.6secs |
| **Moberg Test w/o Vision**[4] | Unable to complete | 20.8secs | Unable to complete | 23.7secs |
| **Object Identification** | 0/12 | 11/12 | 0/12 | 11/12 |
| **Carroll Test**[5] | 83/96 | N/A | 86/96 | N/A |

All scores reflect testing conducted at the time points closest to fMRI grasp data collections. When available, normative values are reported along with associated references. Alternatively, scores are reported for the non-transplanted right hand, if available. Note, however, that the right hand was also injured and underwent multiple surgeries that have compromised both sensory and motor functions. [1]Tested on volar distal tips of thumb, index and small fingers (Mackinnon et al., 2010). [2]Stimuli were applied to the volar surfaces of the tips of the thumb, index and little fingers. Performances reflect diminished light touch (Hunter et al., 1995). [3]Values reflect average error computed across 15 locations distributed across the palm and all five digits (Noordenbos, 1972). [4]These values indicate diminished protective sensation (Amirjani et al., 2007). [5](Carroll, 1965).

### Grasp kinematics

The following kinematic variables are defined: movement time (MT), peak grip aperture (pGA); time to peak grip aperture (ttpGA); peak transport velocity (pV); time to peak transport velocity (ttpV).

***DR's grasp kinematics.*** The atypical aspects of DR's reach-to-grasp control are high pV, which exceeded the control group's upper 95% CI during both

Tests [62.60 to 53.22 cm/s, Z: 2.52 and 1.18, Controls: 44.87 ± 7.05 (SD) cm/s, CI: 37.47 – 52.27], and earlier ttpV than the control's in Test 1. By contrast, all other kinematic variables assessed in DR are within the 95% CIs of healthy controls at both 26 and 41mths post-transplant, and those that reflect grasp preshaping more closely approximate the control mean during the second testing session (**Table 2)**.

**Table 2**. *Reach-to-grasp variables for the left hand of control subjects and D.R.'s affected hand, assessed at 26 and 41mths post-transplant.*

| Variables | Control ± SD (95%CI) | D.R. 26 | D.R. 41 |
|---|---|---|---|
| MT (s) | 0.96 ± 0.19 (0.76 – 1.16) | **0.85** | **1.16** |
| pGA (cm) | 8.90 ± 1.13 (7.72 – 10.09) | **10.02** | **9.24** |
| ttpGA (%) | 63.20 ± 10.84 (53.01 – 73.39) | **49.21** | **67.25** |
| pV (cm/s) | 44.87 ± 7.05 (37.47 – 52.27) | **62.60‡** | **53.22‡** |
| ttpV (%) | 35.18 ± 7.16 (27.66 – 42.70) | **21.24§** | **41.38** |

Values are means ± SD for six control subjects, with the 95% CI in parenthesis. Single measures are presented for each assessment of D.R. ‡ indicates values above and § values below the 95% CI of the control group. MT, Movement Time; pGA, Peak Grip Aperture; ttpGA, Time to Peak Grip Aperture; pV, Peak Transport Velocity; ttpV, Time to Peak Transport Velocity.

More precisely, DR's mean pGA decreased between Tests [10.02 and 9.24 cm, Z: 0.99 and 0.30, Controls: 8.90 ± 1.13 (SD) cm, CI: 7.72 – 10.09], consistent with preshaping that more closely matches the sizes of target objects, thereby leaving smaller margins for error. Also, at Test 2, the ttpGA occurs later in the reaching movement [49.21 and 67.25 %, Z: -1.29 and 0.37, Controls: 63.20 ± 10.84 (SD) %, CI: 53.01 – 73.39], as does the ttpV [21.24 and 41.38%, Z: -1.95 and 0.87, Controls: 35.18 ± 7.16 (SD) %, CI: 27.66 – 42.70]. These temporal changes in grasp control indicate that DR is spending less time preshaping the hand during the deceleration phase of reaching; a change that is consistent with decreased reliance on feedback-based control.

To better understand the nature of DR's atypical hand velocity measures, we performed two additional analyses. First, we computed hand velocity at different percentages of movement time, focusing on the approach phase. Second, we computed a spatial trajectory curvature index (IC), a/b, where a is the maximal normal distance from the path to a straight line joining start and

end points, and b is the straight-line distance. If IC = 0, the trajectory is a perfect straight line; if IC = 1, the trajectory is closer to circular.

Table 3 shows that DR continues to move with a greater hand velocity relative to controls even during the final approach phases of his grasping movements, and that the spatial trajectories of his movements have more curvature than those of controls. We interpret these data as consistent with the use of a more ballistic movement strategy. Such a strategy may minimize the influence of noisy somatosensory and kinesthetic feedback.

**Table 3**. *Hand velocity during approach and index of curvature of the hand trajectory.*

| Variables | Control ± SD (95%CI) | D.R.26 | D.R.41 |
|---|---|---|---|
| V at 60% (cm/s) | 24.65 ± 5.96 (18.39 – 30.91) | **32.01‡** | **29.17** |
| V at 80% (cm/s) | 11.66 ± 3.58 (7.90 – 15.42) | **12.11** | **12.62** |
| V at 95% (cm/s) | 5.88 ± 1.06 (4.77 – 6.99) | **9.48‡** | **7.81‡** |
| V at 100% (cm/s) | 4.25 ± 0.64 (3.58 – 4.92) | **6.72‡** | **5.08‡** |
| IC | 0.0049 ± 0.0008 (0.0041 – 0.0058) | **0.0071‡** | **0.0060‡** |

IC: index of curvature. V = hand velocity at different percentages of movement time.

**Grasp fMRI**

***DR's grasp-selectivity over time.*** At 26mths post-transplant, the contrast Grasp > Touch reveals a relatively large cluster of significant activity within DR's contralateral central sulcus extending rostrally into his precentral gyrus and caudally through the post-central gyrus (primary sensorimotor cortex, SMC) into the aIPC (**Fig 2A**). We refer to this area of activity as the contralateral sensorimotor-anterior intraparietal cortex (SM-aIPC), to indicate that this includes primary motor and somatosensory as well as the anterior intraparietal cortex. Significant grasp-selective responses are also evident bilaterally in medial aspects of the superior frontal gyrus (mSFG) and medial primary sensorimotor cortex (mSMC), the supplementary motor area (SMA), and ipsilaterally within the medial intraparietal cortex (mIPC) and the parietal

operculum (SII, putative secondary somatosensory cortex). Not shown in **Figure 2A**, significant Grasp > Touch activity is also evident along the lateral and inferior edge of the contralateral cerebellum.

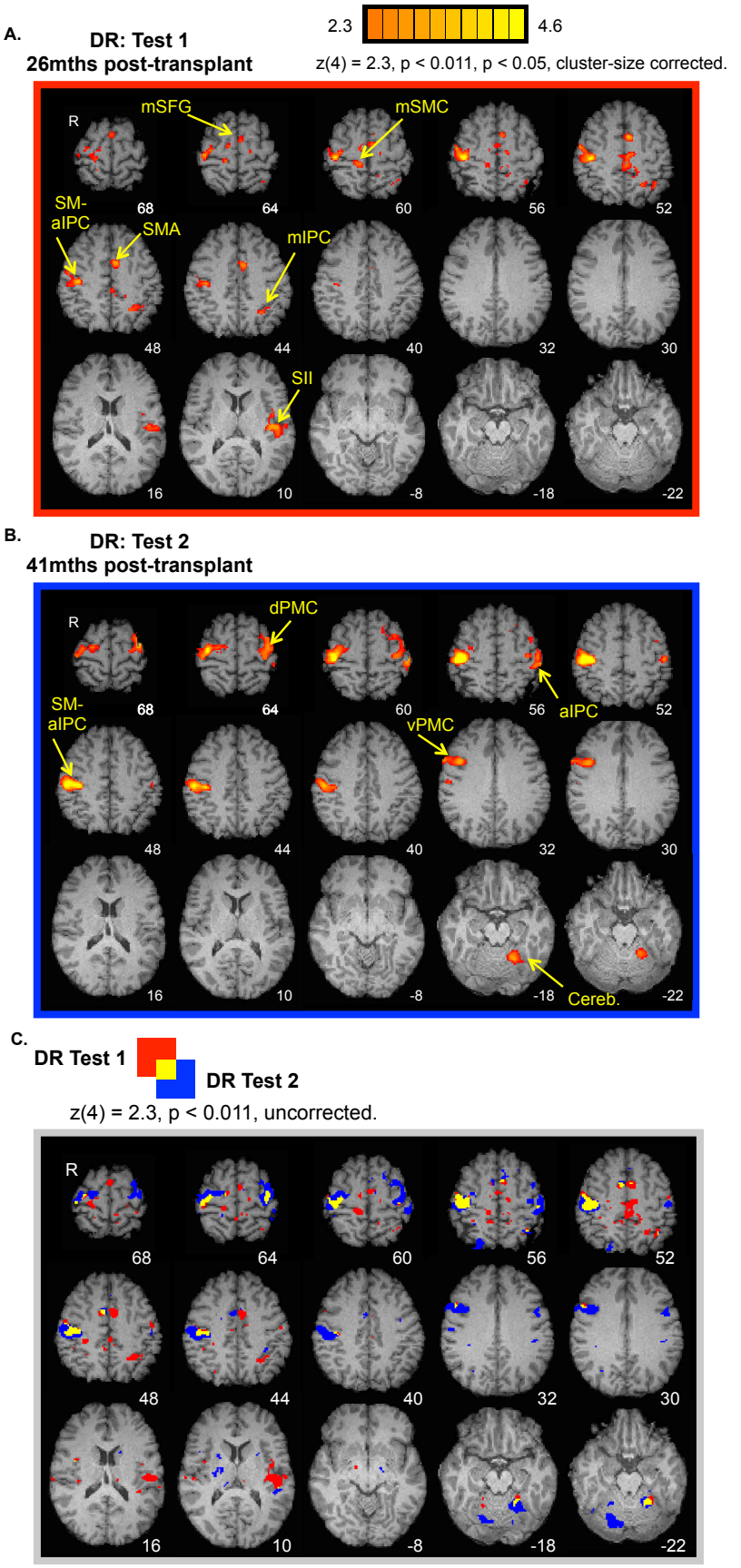


**Fig 2. Grasp-selective responses in DR.** (A) Statistical activation maps showing significant Grasp > Touch responses in DR at Test 1. (B) Same as (A), but at Test 2. (C) These data at uncorrected thresholds: Test 1 (red), Test 2 (blue), and the overlap

(yellow). Abbreviations: medial superior frontal gyrus (mSFG); medial primary sensorimotor cortex (mSMC); primary sensorimotor and anterior intraparietal cortices (SM-aIPC); supplementary motor area (SMA); medial intraparietal cortex (mIPC); secondary somatosensory cortex (SII); dorsal premotor cortex (dPMC); ventral premotor cortex (vPMC); cerebellum (Cereb.).

When tested again at 41mths post-transplant, significant grasp-selective activity within DR's contralateral SM-aIPC is again detected (**Fig 2B**). The results now also reveal significant grasp-selectivity straddling the central sulcus ipsilateral to the grasping – transplanted – hand. This activity comprises two, spatially distinct clusters: one anterior to the central sulcus, overlapping with dorsal premotor cortex (dPMC), and a second cluster posterior to the central sulcus, overlapping with the post-central gyrus and the aIPC. Significant grasp-selective responses are also evident in the contralateral middle frontal gyrus and ventral premotor cortex (vPMC), and the ipsilateral cerebellum (Cereb.).

Single-subject comparisons of fMRI data based on cluster-corrected thresholds can overestimate differences between sessions (Smith et al., 2005). We therefore recomputed the Grasp > Touch contrasts from each session without cluster-wise corrections, binarized these images and overlaid the results on DR's structural scan (**Fig 2C**). Under these conditions, grasp-selective responses appear much more consistent across Tests and include: bilateral aIPC, dPMC and the SMA, contralateral vPMC, and the ipsilateral cerebellum (**yellow regions, Fig 2C**). With the exception of the SMA, all of these areas show more statistically robust grasp-selectivity at 41mths. Conversely, those areas that show little evidence for replication across Tests – mSFG, mSMC, mIPC, SII – are identified at 26mths only.

To summarize, our results are consistent with the hypothesis that skilled, coordinated grasping with a transplanted hand relies on the functions of the aIPC and other key nodes of the extended sensorimotor network known to play an important role in hand control. Across both Tests, grasping with the transplanted hand preferentially activates contralateral aIPC and vPMC, bilateral dPMC and the SMA, and the ipsilateral cerebellum. Further, our data suggest that over time grasping is associated with a more consolidated set of

brain areas. A number of areas that are significantly activated at 26mths are no longer detected at 41mths. These changes accompany more robust ipsilateral recruitment of aIPC, dorsal premotor cortex, and the cerebellum.

***DR's grasp-selectivity compared with healthy controls.*** In order to determine whether DR's grasp-selective results fall within the range of normal individual variability, we show the single-subject-level results from our cohort of healthy controls as the number of subjects per voxel (min. one individual) who show significant Grasp > Touch activity (at the same single-subject statistical thresholds that are applied to DR's data, **Fig 3A**). In addition to contralateral sensorimotor cortex, these results reveal bilateral aIPC, dPMC, SMA, basal ganglia (BG), cerebellum, and contralateral vPMC.

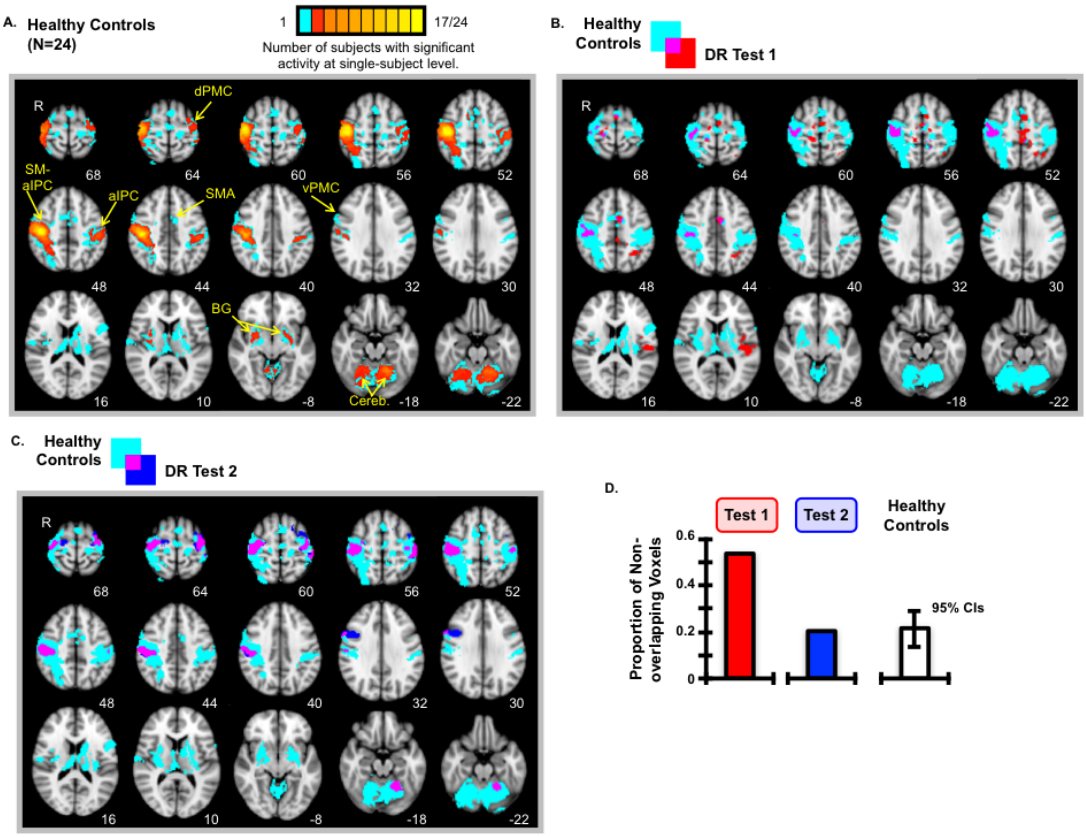


**Fig 3. Grasp-selective responses in healthy controls compared with DR.** (A) Voxel-wise results showing the number of subjects with significant activity for Grasp versus Touch at single-subject thresholds. To provide a clear view of the absolute minimum end of this range, voxels identified in a single control participant are shown in cyan. (B) These same results thresholded at a minimum of one participant (cyan), shown with DR's significant grasp-related activity from Test 1 (red) and the overlap (magenta). (C) Same as (B), but with DR's data from Test 2 (blue). (D) The proportions of active voxels in DR at Tests 1 and 2 that are non-overlapping with the results of at least one control participant, and the control group mean proportion of

active voxels that are non-overlapping with the results of at least one other control participant. Abbreviations: primary sensorimotor and anterior intraparietal cortices (SM-aIPC); anterior intraparietal cortex (aIPC); supplementary motor area (SMA); dorsal premotor cortex (dPMC); ventral premotor cortex (vPMC); basal ganglia (BG); cerebellum (Cereb.).

To visualize common and distinct activity between these and patient DR's data, the single-subject-overlap results from healthy controls are set to a minimum threshold of one subject, binarized and then overlaid with DR's thresholded results from either Test (**Fig 3B and C).** At 26mths post-transplant, DR's grasp-selective activity that overlaps with the probable range of normal grasp-selective responses is restricted to contralateral primary sensorimotor and the aIPC, and the SMA. Conversely, at 41mths post-transplant, DR's pattern of grasp-selectivity now includes ipsilateral dPMC, aIPC, and cerebellar cortices, all of which are identified as within the range of normative responses.

DR's contralateral vPMC at 41mths partly overlaps with the location of activity seen in two healthy controls, and thus may also be considered within our estimate of the range of normative responses. Notably, however, the majority of active voxels in DR in vPMC are non-overlapping with the control's data from this region. This suggests that the level – extent and strength – of functional recruitment of the contralateral vPMC for grasping in DR at 41mths exceeds our normative estimates. We return to this result in our Discussion.

Figure 3D shows the total number of active voxels in DR at Tests 1 and 2 that are non-overlapping with at least one control participant's thresholded activity, expressed as a proportion of the total number of active voxels in DR at each Test, respectively. For comparison, we computed a similar metric for each individual control. Figure 3D shows the group mean proportion of active voxels in single-level control participant's thresholded data maps that are non-overlapping with at least one other control participant's data, with 95% confidence intervals. This provides an estimate of the probable range of activity that is unique to a single individual's data – non-overlapping with any other participant's data from our group.

At 26mths, 53.7% of the total volume of thresholded voxels in DR is non-overlapping with the thresholded activity of at least one control participant. This result is outside the 95% CIs of healthy controls. Two areas stand out, in particular: mIPC and SII. Conversely, at 41mths the proportion of activity in DR that does not overlap with at least one control participant's data drops to 20.4%, to within the 95% CIs of our controls. These results complement our qualitative observations detailed above, and suggest that between 26 and 41mths post-transplant DR's grasp-selective responses are restored to within the range of measures defined by healthy controls.

***DR's grasp-selectivity in normatively-defined ROIs.*** To independently and quantitatively evaluate DR's data within and across our two testing sessions, the healthy control group's data are used to define regions-of-interest (ROIs) based on the contrast Grasp > Touch (**Fig 4**). Six ROIs are defined: contralateral SMC and aIPC, two independent clusters within ipsilateral aIPC (one identified as a dorsolateral focus, named i-aIPCd) and the ipsilateral dPMC and cerebellum. The ROI defined as aIPC is identified as a local statistical maximum, contiguous with the same cluster of activity that defines the SMC ROI, but the two ROIs comprise distinct voxels.

We use two methods to evaluate DR's data within these ROIs. First, per ROI, we compute the one-sided, lower-bound 95% CIs around the mean %-BSC values from DR's data from Tests 1 and 2 for the contrast Grasp > Touch. This provides an estimate of whether DR's responses are reliably non-zero in these areas. The method is, however, conservative, given that the degrees of freedom used to calculate the CIs is 4.

According to this method, DR displays significant grasp-selectivity in contralateral SMC at both Tests 1 and 2, and within contralateral aIPC, ipsilateral dPMC, i-aIPCd, and the cerebellum at Test 2. DR's responses at Test 1 nearly reach significance in aIPC, dPMC, and the cerebellum.

Our second method involves a leave-one-subject-out (LOSO) analysis (see Methods, for details) (Esterman et al., 2010). The method permits estimation

of %-BSC effects sizes and 95% CIs from the control group's data per ROI, while reducing the problem of statistical non-independence (Kriegeskorte et al., 2009).

According to this method, for nearly all control-group-defined ROIs[1], the strength of Grasp > Touch responses in DR are within the range of normal responses at Test 1, and exceed this range at Test 2 (**Fig 4**). The exception is during Test 1, within the i-aIPC. Here, DR's mean %-BSC values are below the lower-arm of the 95% CIs estimated from our control's data.

Notably, the LOSO method used here is likely biased, and may underestimate the control group's error estimates – 95% CIs – from ROIs. Individual LOSO GLM results (Supplementary Figure 1), and the locations of the peak Z statistics used to define ROIs (Supplementary Table 1) show little variation. The results closely mirror the results of the full GLM analyses. While keeping consistent with our method used to evaluate DR's data based on the full group GLM, the use of peak statistics to define ROIs in our LOSO analyses may have biased these results; ROI selection is closely guided by the results of the full group model (for discussion, see Esterman et al., 2010). For these reasons, we choose not to emphasize the apparent hyper-activity seen in DR at Test 2.

To summarize, we use two methods to evaluate DR's responses in control-group-defined ROIs, one that is likely too conservative, and the other that is likely too liberal. The findings intersect, however, and reveal that by 41mths post-transplant DR demonstrates a pattern of grasp-selectivity that is within the normal range of responses defined by healthy controls.

---

[1] In the full group GLM aIPC is identified as a local maximum, contiguous with but distinct from the voxels that comprise the SMC ROI. Conversely, in 7/24 LOSO GLM results, the voxels overlapping with aIPC do not constitute an independent, local maximum. As such, the control group's mean and 95% CIs for aIPC are computed on the basis of 17 control participant's data. Similarly, in the full model i-aIPCd is identified as independent from i-aIPC. Conversely, the two ROIs form a contiguous cluster in 6/24 LOSO GLM results. An independent peak for i-aIPCd is not identifiable. As such, the mean and 95% CIs estimates for i-aIPCd are based on the data from 18 controls. All other results are based on 24 controls.

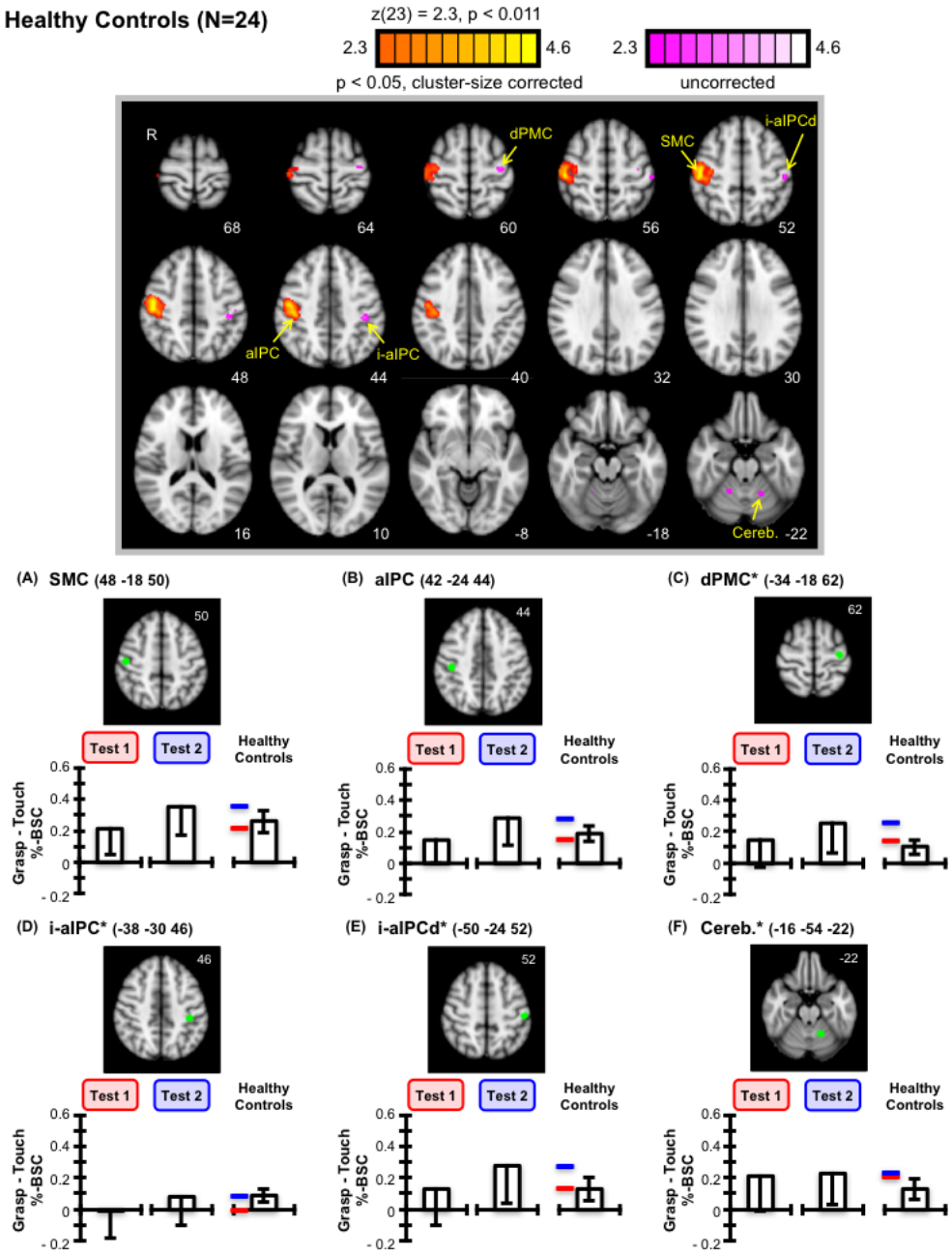


**Fig 4. DR's grasp responses within control-group-defined ROIs**. The control-group-averaged results from the contrast Grasp > Touch (top panel). Six ROIs are defined: sensorimotor cortex (SMC), anterior intraparietal cortex (aIPC), two ROIs within ipsilateral anterior intraparietal cortex (i-aIPC, and a region dorsolateral to this, i-aIPCd), ipsilateral dorsal premotor cortex (dPMC), and ipsilateral cerebellum (Cereb.). The * indicates those regions defined at uncorrected thresholds. From these ROIs, DR's data from either Test are extracted, expressed as the mean %-BSC values for the contrast Grasp > Touch. Error bars reflect one-sided 95% confidence intervals. Also shown for each ROI are the control group %-BSC estimates using the LOSO method (see Methods: ROI analyses), with 95% CIs. To facilitate comparisons, the red and blue lines indicate DR's mean responses at Tests 1 and 2, respectively.

**fMRI sensorimotor mapping**

As shown in amputees (Hamzei et al., 2001; Bogdanov et al., 2012; Philip and Frey, 2014), and in a transplant recipient soon after surgery (Frey et al., 2008), DR exhibits increased activity of the ipsilateral primary sensorimotor hand territory during movements of his natural right hand even at 44mths post-surgery. These responses occur in the very same region that responds during movements of his left, transplanted hand (**Fig 5**).

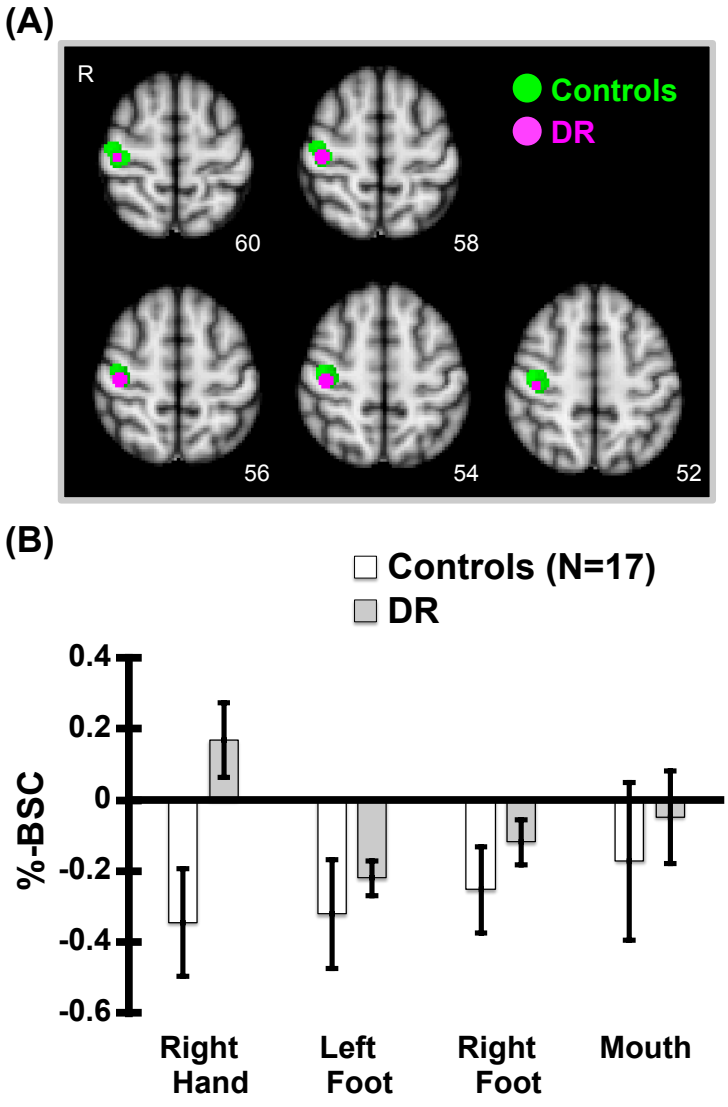


**Fig 5. Responses to hand, feet, and lip movements in right primary sensorimotor cortex.** (A) Right primary sensorimotor cortex ROIs are defined in each individual subject and in DR by movements of the left/transplanted hand. DR's ROI is shown in magenta and controls are shown in green. (B) Mean percent BOLD signal change (%-BSC) values are extracted from ROIs for each of the other body-part movement conditions, shown for DR (grey) and the control's group-average (white). Error bars for controls indicate 95% confidence intervals, and for DR, standard deviations.

## DISCUSSION

Our data reveal for the first time that even after more than a decade of living as an amputee the normative functional brain organization responsible for the visual control of grasping can be restored following hand transplantation. Improved grasp performance parallels the normalization of grasp-selective fMRI responses in the aIPC, premotor and cerebellar cortices. Functional normalization of this network for visually guided grasping develops despite prevailing amputation-related functional changes in primary sensorimotor cortex (S1/M1) and significant low-level sensory and motor impairments. We conjecture that this brain network supports the restoration of grasp function following hand transplantation primarily through the use of visual feedback to compensate for errors arising from persistent reorganizational changes in S1/M1, and reinnervation errors in regenerating peripheral nerves.

### Largely normal grasp kinematics despite persistent sensorimotor impairments

Improvements in basic sensory and motor abilities following hand transplantation are variable and continue over many years (Breidenbach et al., 2008; Landin et al., 2012; Shores et al., 2015). At 26 and 41mths post-surgery, DR continues to display moderate-to-severe limitations across a variety of basic sensory and motor evaluations. In spite of these limitations his reach-to-grasp kinematics are remarkably typical, a pattern that is consistent with recent data from other transplant recipients (Huchon et al., 2016). With the exception of peak reach velocity, all other kinematic measures of DR's reach and grasp performance are within the 95% confidence intervals defined by healthy controls. His peak reach velocity is atypically high. Although speculative, higher peak velocity may reflect the use of a more ballistic movement strategy, heavily reliant on feed-forward control mechanisms. This would minimize opportunities for the influence of noisy sensory feedback. Clearly, however, more work is needed to evaluate this speculation.

Of particular note, DR's timing and scaling of grip aperture become increasingly similar to controls at 41mths. At 26mths, peak grip aperture

tended to exceed that of controls, and was achieved earlier in the reach. This may reflect compensation for limitations in hand control. Larger grip aperture allows a greater margin for error in hand preshaping, and the early time to reach peak aperture enables more time to use visual feedback to adjust the grasp during the deceleration phase of the movement. By 41mths, peak grip aperture and its temporal organization more closely approximate the mean of the control group. Together, these data indicate increasing normalization of the control of hand preshaping, a function that has been repeatedly ascribed to the aIPC and interconnected regions of the premotor cortex (Jeannerod et al., 1995; Castiello, 2005; Grafton, 2010; Davare et al., 2011). Our results provide critical new support for this model.

**Normalization of grasp-selective fMRI responses**

As early as 26mths post-transplant, DR exhibits grasp-selective responses in contralateral sensorimotor cortex and aIPC. By 41mths, grasp-selectivity is more robust in these areas, and is now also detected in the ipsilateral aIPC, cerebellum, and premotor cortices; the same network of areas showing grasp-selectivity in healthy controls. The data reveal that by 41mths post-surgery, DR's fMRI responses associated with grasping are within the range of normal variation defined by controls.

This evidence is consistent with the possibility that DR is recruiting the same regions that are likely to have controlled grasping with his own hand prior to amputation. Our ROI results provide further support for this interpretation. At 26mths, DR shows significant grasp-selectivity in the control-group-defined SMC, and by 41mths, responses in the control-group-defined aIPC, dorsal premotor cortex and cerebellum reach significance.

DR's data also indicate that over time the network of brain areas associated with grasping is refined. Specifically, at 26 but not at 41mths DR shows grasp-selective responses in numerous other brain areas (mSMC, mIPC, SII) not reliably identified in controls. These results indicate that atypically organized grasp-selective responses are evident early and resolve

over time, and as noted above, these changes parallel improvements in the control of hand preshaping.

An important part of the current work is the demonstration of substantial individual variation in the network of regions in healthy adults that exhibit grasp-selective responses. These differences can be obscured using group-averaged methods alone, thereby making comparative interpretations with individual patient data problematic. In this case, we would conclude that DR shows a predominately atypical pattern. This would be mistaken.

Our data define the aIPC, dPMC and vPMC, and the cerebellum as part of the normative cortical network selective for grasping in healthy controls. The involvement of these areas in grasp control is consistent with a range of evidence from multiple domains (Castiello, 2005; Grafton, 2010; Davare et al., 2011).

Increased cerebellar activity may reflect greater reliance on predictive, feed-forward control in DR. The cerebellum is widely held to play an essential role in feed-forward control mechanisms (Wolpert et al., 1995; Wolpert et al., 1998; Flanagan et al., 2003; Miall and King, 2008). This interpretation is consistent with our account of DR's atypically high peak velocities as related to a greater reliance on feed-forward control. Alternatively, non-synergistic control of the fingers for grasping may place greater demands on motor function, and this may lead to increased activity in the contralateral SMC and ipsilateral cerebellum. Future work is needed to distinguish these possibilities.

**The Compensatory Control Hypothesis**

We began this project with a simple question: how can a transplant recipient exhibit relatively normal reach-to-grasp kinematics in spite of significant limitations in basic sensorimotor functions? Our results suggest that the answer involves compensation enabled by a network of brain areas upstream from S1/M1, including the aIPC, the dorsal and ventral premotor cortices, and the cerebellum. We speculate that this compensatory control is accomplished primarily through the use of visual feedback.

Monkey area AIP located at the anterior extent of the intraparietal sulcus is densely interconnected with ventral premotor area F5 in the arcuate sulcus (Sakata and Taira, 1994; Rizzolatti and Luppino, 2001), and together these regions constitute a circuit that transforms visual information about the spatial properties of objects (e.g., shape) to motor programs for configuring the hand during grasping (Jeannerod, 1981; Jeannerod et al., 1995; Schaffelhofer and Scherberger, 2016). There are cells in area AIP with visual response properties consistent with a role in monitoring movements of the hand during grasping, in addition to those tuned to object properties (Sakata et al., 1995; Gardner et al., 1999; Murata et al., 2000).

Convergent evidence suggests that human aIPC and premotor cortex comprise a functionally similar circuit (Jeannerod et al., 1995; Castiello, 2005; Culham and Valyear, 2006; Grafton, 2010; Davare et al., 2011). Perturbation studies reveal that TMS to the aIPC interferes with the ability to compensate for errors in the motor program on the basis of visual feedback, suggesting that the aIPC plays a key role in this updating function (Tunik et al., 2005; Rice et al., 2006). Specifically, the model supported by this work implicates the aIPC as critical for integrating the motor commands that specify the spatiotemporal parameters of intended actions with incoming visual information online, after actions are initiated, to rapidly detect and adjust for differences between them. We suggest that this is precisely the kind of corrective function that is likely to be essential for controlling a transplanted hand with limited and noisy sensory feedback.

Our data also reveal the involvement of bilateral dPMC and ipsilateral cerebellum. The dPMC is commonly identified in fMRI studies of grasping (see meta-analysis, Valyear et al., 2017), and TMS to dPMC disrupts the timing of grip and lift features of grasp control (Davare et al., 2006). Like monkey area AIP, dorsal premotor area F2 in monkeys appears to play an important role in monitoring hand actions on the basis of visual feedback (Raos et al., 2004).

The cerebellum is essential for feed-forward control (Wolpert et al., 1995; Wolpert et al., 1998; Flanagan et al., 2003; Miall and King, 2008), as noted earlier, and has been strongly implicated in motor skill learning (Wolpert et al., 2001). In monkeys, the cerebellum and basal ganglia have direct inputs to area AIP (Clower et al., 2005), and together, this circuit may be essential for enabling rapid corrective adjustments to ongoing actions.

On the basis of our new findings, and in light of these prior data, we hypothesize that the aIPC, d- and vPMC, and the cerebellum constitute a core network of brain areas that together enable normative grasp performance with a transplanted hand by using vision to correct for errors in the initial motor program, and from noisy somatosensory and kinesthetic feedback, that arise as a consequence of incomplete sensory recovery.

We further conjecture that these same areas are important for the flexible, compensatory control of the hand in other circumstances where modality-specific inputs are limited, such as with peripheral neuropathies and tool use. Consistently, using handheld tools reliably activates the aIPC and premotor areas (Jacobs et al., 2010; Valyear et al., 2012; Gallivan et al., 2013; Brandi et al., 2014).

Recent unpublished data suggest that visual feedback during grasping is of significant benefit to DR (Mattos et al., 2016). Grasping a glowing object in the dark without vision of his moving limb negatively affects his performance. Conversely, however, other research shows that forcing bilateral transplant recipients to grasp remembered targets by removing vision entirely does not substantially compromise their grasp control (Huchon et al., 2016). Although, one patient was entirely unable to complete the task (for one hand) without vision. More work is necessary to understand the role of vision in grasp control with a transplanted hand.

**Alternate interpretations**

Our hypothesis stated above may be said to underplay other aspects of our results. First, our data identify atypical grasp-selectivity in DR early, at

26mths. In particular, grasping preferentially activates an area in DR's posterior and medial intraparietal cortex (mIPC), and within the parietal operculum, likely overlapping with SII. Both responses are seen ipsilateral to his transplanted hand. No single control participant shows activity in either of these areas.

The significance of these results is unclear. The mIPC is implicated in the control of the arm for reaching (Astafiev et al., 2003; Beurze et al., 2007, 2009), hypothesized to correspond functionally with monkey area MIP (a key component of the parietal reach region) (Vesia and Crawford, 2012; Andersen et al., 2014). Why this area would be selectively active in DR at 26mths, and only ipsilaterally with respect to his acting limb, is puzzling, however.

One reviewer draws attention to recent data that call into question the classic view of separate dedicated parietofrontal systems for reaching versus grasping (Pitzalis et al., 2005; Monaco et al., 2011; Fattori et al., 2017), and notes that ipsilateral engagement in DR may make sense given that as an amputee, this system would have continued to drive the use of his intact limb. Such conditions may promote ipsilateral control following transplantation, at least early on. That is, perhaps DR's ipsilateral mIPC contributes to the control of his transplanted hand, in particular, soon after surgery, during the early stages of his recovery. This hypothesis is speculative, and clarification will require future longitudinal work with other hand transplant recipients.

Likewise, it remains unclear why DR's ipsilateral SII shows early involvement during grasping, and why this resolves over time. In our work with unilateral hand amputees, we find that pure cutaneous sensory stimulation of the remaining digits activates primary sensory cortices bilaterally (Philip et al., 2015). As one interpretation, ipsilateral responses reflect changes in the balance of interhemispheric inhibition brought on by the dramatic decreases in activity contralateral to the missing hand (Calford and Tweedale, 1990; Cohen et al., 1991b; Bogdanov et al., 2012). Although speculative, and underspecified, the ipsilateral responses in SII in DR at 26mths post-transplant may relate to persistent changes in interhemispheric functional

connectivity between secondary somatosensory cortices as a result of chronic hand loss. Future investigations with additional patients will help to better understand the importance of these results.

These aspects of our findings point to a model of grasp recovery after hand transplantation that differs from our emphasis above. While our compensatory control hypothesis focuses on the importance of increasing recruitment of grasp-typical brain areas over time, these results highlight how grasp recovery may also involve decreases in grasp-atypical brain responses over time.

Specifically, these data suggest that early-level recovery involves compensation via recruitment of brain regions that are not typically associated with grasping in healthy controls – i.e. ipsilateral mIPC and SII. This suggests that our compensatory control hypothesis is incomplete. While the restoration of grasp control with a transplanted hand may indeed depend on the lasting recruitment of aIPC, d- and vPMC, and the cerebellum, and the use of vision by this network, temporary early-stage involvement of ipsilateral mIPC and SII may also be important.

Alternatively, this early-stage engagement of grasp-atypical regions may be maladaptive, and reflect a form of functional disorganization. Perhaps it is the gradual dis-involvement of these areas that promotes the recovery of grasp function with time. Further research may tease apart these opposing hypotheses.

Second, DR demonstrates robust grasp-selective responses in vPMC. These responses increase in strength over time, evident only at cluster-size uncorrected levels at 26mths (Fig. 2C), and robustly, at corrected levels by 41mths (Fig. 2B). Additionally, few controls show significant grasp-selective responses in vPMC. This result contrasts with an interpretation of DR's data as uniformly exhibiting increasingly normative brain responses for grasping over time. The level of his vPMC involvement, especially at 41mths, appears atypical.

We speculate that these results relate to the unique motoric demands associated with the control of DR's transplanted hand. Even at 41mths, DR's basic motor functions remain impaired (Table 1), including an inability to individuate the control of his digits, and minimal functionality of the intrinsic muscle groups. These limitations are likely to place higher demands on the motor control of the hand. We hypothesize that such demands may tax the functions of vPMC, in particular.

Two sets of prior evidence motivate this hypothesis. First, monkey data suggest a functional continuum within the AIP-F5 circuit, whereby F5 is more directly responsible for encoding the motoric features of grasp control. Specifically, multidimensional scaling methods reveal that while object-selectivity in AIP best reflects structural object features, selectivity in F5 is better explained by the hand configurations associated with grasping those objects (Murata et al., 2000; Raos et al., 2006; Schaffelhofer and Scherberger, 2016). Second, fMRI studies involving complex manual actions commonly report vPMC involvement (Valyear et al., 2012; Brandi et al., 2014). This contrasts with those studies involving simpler grasping tasks, like the current study, where the vPMC is not commonly identified.

Finally, we recognize that grasp-selectivity in the aIPC in both DR and controls is part of a continuous cluster that spans both post and precentral cortices; separating the aIPC from S1/M1 involvement requires justification. Our rationale is threefold. First, grasp-selectivity in DR and controls overlaps with the aIPC. This is clear from the ventral and posterior extents of these data (Fig. 2 and 4), non-overlapping with the expected locations of S1/M1, and clearly distinct from the focus of peak responses identified via simple finger movements, which is situated within the central sulcus (Fig. 5A). Second, as reviewed above, a wealth of prior data link the aIPC to grasp control. To suggest that our results within the aIPC merely reflect a spread of responses from S1/M1 directly conflicts with this evidence. Third, our results identify the involvement of d- and vPMC, regions that are known to functionally interact with the aIPC during grasping (Davare et al., 2011), and

that are clearly spatially distinct from S1/M1. For these reasons, we feel that discussion of our data showing aIPC involvement as separate from the functional contributions of S1/M1 is justified.

**Implications**

Our results suggest that grasping and the normative functional brain organization governing the control of grasping can be recovered during the first 2-4 years following allogeneic hand transplantation. These findings have positive rehabilitation implications for hand transplant recipients. At the same time, as a single case study, we recognize that the current data must be considered cautiously; generalizability depends on the results of future investigations with additional patients. Nonetheless, this study provides the first available measures of brain function related to the return of grasp control with a transplanted hand. Our results lay the foundation for future research in this area, and provide an invaluable benchmark for which to compare subsequent findings.

## REFERENCES

Almquist E, Eeg-Olofsson O (1970) Sensory-nerve-conduction velocity and two-point discrimmination in sutured nerves. J Bone Joint Surg Am 52:791-796.

Amirjani N, Ashworth NL, Gordon T, Edwards DC, Chan KM (2007) Normative values and the effects of age, gender, and handedness on the Moberg Pick-Up Test. Muscle Nerve 35:788-792.

Andersen RA, Andersen KN, Hwang EJ, Hauschild M (2014) Optic ataxia: from Balint's syndrome to the parietal reach region. Neuron 81:967-983.

Astafiev SV, Shulman GL, Stanley CM, Snyder AZ, Van Essen DC, Corbetta M (2003) Functional organization of human intraparietal and frontal cortex for attending, looking, and pointing. J Neurosci 23:4689-4699.

Beurze SM, de Lange FP, Toni I, Medendorp WP (2007) Integration of target and effector information in the human brain during reach planning. J Neurophysiol 97:188-199.

Beurze SM, de Lange FP, Toni I, Medendorp WP (2009) Spatial and effector processing in the human parietofrontal network for reaches and saccades. J Neurophysiol 101:3053-3062.

Biddiss E, Beaton D, Chau T (2007) Consumer design priorities for upper limb prosthetics. Disabil Rehabil Assist Technol 2:346-357.

Binkofski F, Dohle C, Posse S, Stephan KM, Hefter H, Seitz RJ, Freund HJ (1998) Human anterior intraparietal area subserves prehension: a combined lesion and functional MRI activation study. Neurology 50:1253-1259.

Bogdanov S, Smith J, Frey SH (2012) Former hand territory activity increases after amputation during intact hand movements, but is unaffected by illusory visual feedback. Neurorehabil Neural Repair 26:604-615.

Brandi ML, Wohlschlager A, Sorg C, Hermsdorfer J (2014) The neural correlates of planning and executing actual tool use. J Neurosci 34:13183-13194.

Breidenbach WC, Gonzales NR, Kaufman CL, Klapheke M, Tobin GR, Gorantla VS (2008) Outcomes of the first 2 American hand transplants at 8 and 6 years posttransplant. J Hand Surg Am 33:1039-1047.

Brenneis C, Loscher WN, Egger KE, Benke T, Schocke M, Gabl MF, Wechselberger G, Felber S, Pechlaner S, Margreiter R, Piza-Katzer H, Poewe W (2005) Cortical motor activation patterns following hand transplantation and replantation. J Hand Surg Br 30:530-533.

Calford MB, Tweedale R (1990) Interhemispheric transfer of plasticity in the cerebral cortex. Science 249:805-807.

Carroll D (1965) A Quantitative Test of Upper Extremity Function. J Chronic Dis 18:479-491.

Castiello U (2005) The neuroscience of grasping. Nat Rev Neurosci 6:726-736.

Clower DM, Dum RP, Strick PL (2005) Basal ganglia and cerebellar inputs to 'AIP'. Cereb Cortex 15:913-920.

Cohen LG, Bandinelli S, Findley TW, Hallett M (1991a) Motor reorganization after upper limb amputation in man. A study with focal magnetic stimulation. Brain 114 ( Pt 1B):615-627.

Cohen LG, Bandinelli S, Topka HR, Fuhr P, Roth BJ, Hallett M (1991b) Topographic maps of human motor cortex in normal and pathological conditions: mirror movements, amputations and spinal cord injuries. Electroencephalogr Clin Neurophysiol Suppl 43:36-50.

Culham JC, Valyear KF (2006) Human parietal cortex in action. Curr Opin Neurobiol 16:205-212.

Culham JC, Danckert SL, DeSouza JF, Gati JS, Menon RS, Goodale MA (2003) Visually guided grasping produces fMRI activation in dorsal but not ventral stream brain areas. Exp Brain Res 153:180-189.

Davare M, Kraskov A, Rothwell JC, Lemon RN (2011) Interactions between areas of the cortical grasping network. Curr Opin Neurobiol 21:565-570.

Davare M, Andres M, Cosnard G, Thonnard JL, Olivier E (2006) Dissociating the role of ventral and dorsal premotor cortex in precision grasping. J Neurosci 26:2260-2268.

Davare M, Andres M, Clerget E, Thonnard JL, Olivier E (2007) Temporal dissociation between hand shaping and grip force scaling in the anterior intraparietal area. J Neurosci 27:3974-3980.

Duvernoy HM (1999) The Human Brain: Surface, Three-Dimensional Sectional Anatomy with MRI, and Blood Supply, Second, completely revised and enlarged edition Edition. New York: Springer-Verlag Wien.

Elbert T, Flor H, Birbaumer N, Knecht S, Hampson S, Larbig W, Taub E (1994) Extensive reorganization of the somatosensory cortex in adult humans after nervous system injury. Neuroreport 5:2593-2597.

Esterman M, Tamber-Rosenau BJ, Chiu YC, Yantis S (2010) Avoiding non-independence in fMRI data analysis: leave one subject out. Neuroimage 50:572-576.

Fattori P, Breveglieri R, Bosco A, Gamberini M, Galletti C (2017) Vision for Prehension in the Medial Parietal Cortex. Cereb Cortex 27:1149-1163.

Flanagan JR, Vetter P, Johansson RS, Wolpert DM (2003) Prediction precedes control in motor learning. Curr Biol 13:146-150.

Flor H, Diers M, Andoh J (2013) The neural basis of phantom limb pain. Trends Cogn Sci 17:307-308.

Flor H, Elbert T, Knecht S, Wienbruch C, Pantev C, Birbaumer N, Larbig W, Taub E (1995) Phantom-limb pain as a perceptual correlate of cortical reorganization following arm amputation. Nature 375:482-484.

Frey SH (2014) Why Brain Science is Essential to the Success of Hand Allotransplantation. In: The Science of Reconstructive Transplantation. (Brandacher G, ed), pp 361-375. New York: Springer.

Frey SH, Vinton D, Norlund R, Grafton ST (2005) Cortical topography of human anterior intraparietal cortex active during visually guided grasping. Brain Res Cogn Brain Res 23:397-405.

Frey SH, Bogdanov S, Smith JC, Watrous S, Breidenbach WC (2008) Chronically deafferented sensory cortex recovers a grossly typical

organization after allogenic hand transplantation. Curr Biol 18:1530-1534.
Gaine WJ, Smart C, Bransby-Zachary M (1997) Upper limb traumatic amputees. Review of prosthetic use. J Hand Surg Br 22:73-76.
Gallivan JP, McLean DA, Valyear KF, Culham JC (2013) Decoding the neural mechanisms of human tool use. Elife 2:e00425.
Gardner EP, Ro JY, Debowy D, Ghosh S (1999) Facilitation of neuronal activity in somatosensory and posterior parietal cortex during prehension. Exp Brain Res 127:329-354.
Garraghty PE, Kaas JH (1991) Large-scale functional reorganization in adult monkey cortex after peripheral nerve injury. Proc Natl Acad Sci U S A 88:6976-6980.
Giraux P, Sirigu A, Schneider F, Dubernard JM (2001) Cortical reorganization in motor cortex after graft of both hands. Nat Neurosci 4:691-692.
Grafton ST (2010) The cognitive neuroscience of prehension: recent developments. Exp Brain Res 204:475-491.
Hamzei F, Liepert J, Dettmers C, Adler T, Kiebel S, Rijntjes M, Weiller C (2001) Structural and functional cortical abnormalities after upper limb amputation during childhood. Neuroreport 12:957-962.
Hernandez-Castillo CR, Aguilar-Castaneda E, Iglesias M, Fernandez-Ruiz J (2016) Motor and sensory cortical reorganization after bilateral forearm transplantation: Four-year follow-up fMRI case study. Magn Reson Imaging 34:541-544.
Huchon L, Badet L, Roy AC, Finos L, Gazarian A, Revol P, Bernardon L, Rossetti Y, Morelon E, Rode G, Farne A (2016) Grasping objects by former amputees: The visuo-motor control of allografted hands. Restor Neurol Neurosci 34:615-633.
Hunter JM, Callahan AD, Mackin EJ (1995) In: Rehabilitation of the hand: surgery and therapy: Mosby, 1990.
Jacobs S, Danielmeier C, Frey SH (2010) Human anterior intraparietal and ventral premotor cortices support representations of grasping with the hand or a novel tool. J Cogn Neurosci 22:2594-2608.
Jeannerod M (1981) The neural and behavioral organization of goal-directed movements. New York: Oxford Science Publishers.
Jeannerod M, Arbib MA, Rizzolatti G, Sakata H (1995) Grasping objects: the cortical mechanisms of visuomotor transformation. Trends Neurosci 18:314-320.
Johnson KO, Phillips JR (1981) Tactile spatial resolution. I. Two-point discrimination, gap detection, grating resolution, and letter recognition. J Neurophysiol 46:1177-1192.
Karl A, Birbaumer N, Lutzenberger W, Cohen LG, Flor H (2001) Reorganization of motor and somatosensory cortex in upper extremity amputees with phantom limb pain. J Neurosci 21:3609-3618.
Kriegeskorte N, Simmons WK, Bellgowan PS, Baker CI (2009) Circular analysis in systems neuroscience: the dangers of double dipping. Nat Neurosci 12:535-540.
Landin L, Bonastre J, Casado-Sanchez C, Diez J, Ninkovic M, Lanzetta M, del Bene M, Schneeberger S, Hautz T, Lovic A, Leyva F, Garcia-de-

Lorenzo A, Casado-Perez C (2012) Outcomes with respect to disabilities of the upper limb after hand allograft transplantation: a systematic review. Transpl Int 25:424-432.

Lanzetta M, Perani D, Anchisi D, Rosen B, Danna M, Scifo P, Fazio F, Lundborg G (2004) Early use of artificial sensibility in hand transplantation. Scand J Plast Reconstr Surg Hand Surg 38:106-111.

Lieberman MD, Cunningham WA (2009) Type I and Type II error concerns in fMRI research: re-balancing the scale. Soc Cogn Affect Neurosci 4:423-428.

Lotze M, Flor H, Grodd W, Larbig W, Birbaumer N (2001) Phantom movements and pain. An fMRI study in upper limb amputees. Brain 124:2268-2277.

Lundborg G, Rosen B (2007) Hand function after nerve repair. Acta Physiol (Oxf) 189:207-217.

Mackinnon SE, Fox IK, Yee A, Kahn L, Law J-Z, Brown JM (2010) Peripheral nerve surgery: a resource for physicians. In: Washington University School of Medicine (http://nervesurgery.wustl.edu/).

Makin TR, Scholz J, Henderson Slater D, Johansen-Berg H, Tracey I (2015) Reassessing cortical reorganization in the primary sensorimotor cortex following arm amputation. Brain 138:2140-2146.

Makin TR, Scholz J, Filippini N, Henderson Slater D, Tracey I, Johansen-Berg H (2013) Phantom pain is associated with preserved structure and function in the former hand area. Nat Commun 4:1570.

Mattos D, Baune N, Philip BA, Valyear KF, Kaufman C, Frey SH (2016) Former unilateral amputees exhibit bilateral differences in the control of reach to grasp actions. 2016 Society for Neuroscience Meeting Planner, Program No. 56.16.

Merzenich MM, Nelson RJ, Stryker MP, Cynader MS, Schoppmann A, Zook JM (1984) Somatosensory cortical map changes following digit amputation in adult monkeys. J Comp Neurol 224:591-605.

Miall RC, King D (2008) State estimation in the cerebellum. Cerebellum 7:572-576.

Monaco S, Cavina-Pratesi C, Sedda A, Fattori P, Galletti C, Culham JC (2011) Functional magnetic resonance adaptation reveals the involvement of the dorsomedial stream in hand orientation for grasping. J Neurophysiol 106:2248-2263.

Murata A, Gallese V, Luppino G, Kaseda M, Sakata H (2000) Selectivity for the shape, size, and orientation of objects for grasping in neurons of monkey parietal area AIP. J Neurophysiol 83:2580-2601.

Neugroschl C, Denolin V, Schuind F, Van Holder C, David P, Baleriaux D, Metens T (2005) Functional MRI activation of somatosensory and motor cortices in a hand-grafted patient with early clinical sensorimotor recovery. Eur Radiol 15:1806-1814.

Noordenbos W (1972) The sensory stimulus and the verbalisation of the response: the pain problem. In: Neurophysiology Studied in Man, International Congress Series No. 253 (Somjen JJ, ed), pp 207-214. Amsterdam: Excerpta Medica.

Oldfield RC (1971) The assessment and analysis of handedness: the Edinburgh inventory. Neuropsychologia 9:97-113.
Philip BA, Frey SH (2014) Compensatory changes accompanying chronic forced use of the nondominant hand by unilateral amputees. J Neurosci 34:3622-3631.
Philip BA, Valyear KF, Frey SH (2015) Evidence for interhemispheric reorganization in sensory cortex following unilateral upper extremity amputation in humans. 2015 Society for Neuroscience Meeting Planner, Program No. 419.20.
Pitzalis S, Galletti C, Fabiana P, Committeri G, Gaspare G, Fattori P, Sereno M (2005) Functional properties of human visual area V6. Neuroimage 26:S23.
Pons TP, Garraghty PE, Ommaya AK, Kaas JH, Taub E, Mishkin M (1991) Massive cortical reorganization after sensory deafferentation in adult macaques. Science 252:1857-1860.
Ramachandran VS, Rogers-Ramachandran D, Stewart M (1992) Perceptual correlates of massive cortical reorganization. Science 258:1159-1160.
Raos V, Umilta MA, Gallese V, Fogassi L (2004) Functional properties of grasping-related neurons in the dorsal premotor area F2 of the macaque monkey. J Neurophysiol 92:1990-2002.
Raos V, Umilta MA, Murata A, Fogassi L, Gallese V (2006) Functional properties of grasping-related neurons in the ventral premotor area F5 of the macaque monkey. J Neurophysiol 95:709-729.
Rice NJ, Tunik E, Grafton ST (2006) The anterior intraparietal sulcus mediates grasp execution, independent of requirement to update: new insights from transcranial magnetic stimulation. J Neurosci 26:8176-8182.
Rizzolatti G, Luppino G (2001) The cortical motor system. Neuron 31:889-901.
Sakata H, Taira M (1994) Parietal control of hand action. Current Opinion in Neurobiology 4:847-856.
Sakata H, Taira M, Murata A, Mine S (1995) Neural mechanisms of visual guidance of hand action in the parietal cortex of the monkey. Cereb Cortex 5:429-438.
Schaffelhofer S, Scherberger H (2016) Object vision to hand action in macaque parietal, premotor, and motor cortices. Elife 5:e15278.
Shores JT, Brandacher G, Lee WP (2015) Hand and upper extremity transplantation: an update of outcomes in the worldwide experience. Plast Reconstr Surg 135:351e-360e.
Smith SM, Beckmann CF, Ramnani N, Woolrich MW, Bannister PR, Jenkinson M, Matthews PM, McGonigle DJ (2005) Variability in fMRI: a re-examination of inter-session differences. Hum Brain Mapp 24:248-257.
Smith SM, Jenkinson M, Woolrich MW, Beckmann CF, Behrens TE, Johansen-Berg H, Bannister PR, De Luca M, Drobnjak I, Flitney DE, Niazy RK, Saunders J, Vickers J, Zhang Y, De Stefano N, Brady JM, Matthews PM (2004) Advances in functional and structural MR image

analysis and implementation as FSL. Neuroimage 23 Suppl 1:S208-219.
Tiffin J, Asher EJ (1948) The Purdue pegboard; norms and studies of reliability and validity. J Appl Psychol 32:234-247.
Tunik E, Frey SH, Grafton ST (2005) Virtual lesions of the anterior intraparietal area disrupt goal-dependent on-line adjustments of grasp. Nat Neurosci 8:505-511.
Valyear KF, Fitzpatrick AM, McManus EF (2017) The Neuroscience of Human Tool Use. In: Evolution of Nervous Systems, 2 Edition (Kaas J, ed), pp 341-353. Oxford: Elsevier.
Valyear KF, Gallivan JP, McLean DA, Culham JC (2012) fMRI repetition suppression for familiar but not arbitrary actions with tools. J Neurosci 32:4247-4259.
Vesia M, Crawford JD (2012) Specialization of reach function in human posterior parietal cortex. Exp Brain Res 221:1-18.
Wall JT, Kaas JH, Sur M, Nelson RJ, Felleman DJ, Merzenich MM (1986) Functional reorganization in somatosensory cortical areas 3b and 1 of adult monkeys after median nerve repair: possible relationships to sensory recovery in humans. J Neurosci 6:218-233.
Wolpert DM, Ghahramani Z, Jordan MI (1995) An internal model for sensorimotor integration. Science 269:1880-1882.
Wolpert DM, Miall RC, Kawato M (1998) Internal models in the cerebellum. Trends Cogn Sci 2:338-347.
Wolpert DM, Ghahramani Z, Flanagan JR (2001) Perspectives and problems in motor learning. Trends Cogn Sci 5:487-494.
Woolrich MW, Ripley BD, Brady M, Smith SM (2001) Temporal autocorrelation in univariate linear modeling of FMRI data. Neuroimage 14:1370-1386.
Woolrich MW, Behrens TE, Beckmann CF, Jenkinson M, Smith SM (2004) Multilevel linear modelling for FMRI group analysis using Bayesian inference. Neuroimage 21:1732-1747.
Yang TT, Gallen CC, Ramachandran VS, Cobb S, Schwartz BJ, Bloom FE (1994) Noninvasive detection of cerebral plasticity in adult human somatosensory cortex. Neuroreport 5:701-704.

**Supplementary Table 1.**

**LOSO ROI results.** The means and 95% CIs of the MNI coordinates and maximum Z statistic for each ROI defined by the LOSO analyses.

| | (A) SMC | | | | (B) aIPC | | | |
|---|---|---|---|---|---|---|---|---|
| | MNI coordinates | | | Maximum | MNI coordinates | | | Maximum |
| | X | Y | Z | Z statistic | X | Y | Z | Z statistic |
| Mean | 48.25 | -18.92 | 50.50 | 4.99 | 42.12 | -24.00 | 44.12 | 4.21 |
| 95% CI | 0.29 | 0.86 | 0.57 | 0.06 | 0.25 | 0.00 | 0.25 | 0.08 |
| | **(C) dPMC** | | | | **(D) i-aIPC** | | | |
| | MNI coordinates | | | Maximum | MNI coordinates | | | Maximum |
| | X | Y | Z | Z statistic | X | Y | Z | Z statistic |
| Mean | -35.20 | -18.00 | 61.30 | 3.01 | -39.00 | -30.00 | 45.10 | 2.97 |
| 95% CI | 0.43 | 0.00 | 0.42 | 0.05 | 0.43 | 0.00 | 0.43 | 0.06 |
| | **(E) i-aIPCd** | | | | **(F) Cereb.** | | | |
| | MNI coordinates | | | Maximum | MNI coordinates | | | Maximum |
| | X | Y | Z | Z statistic | X | Y | Z | Z statistic |
| Mean | -50.78 | -24.89 | 53.33 | 2.65 | -17.00 | -54.00 | -22.17 | 2.56 |
| 95% CI | 0.50 | 0.61 | 0.90 | 0.26 | 0.43 | 0.00 | 0.24 | 0.06 |

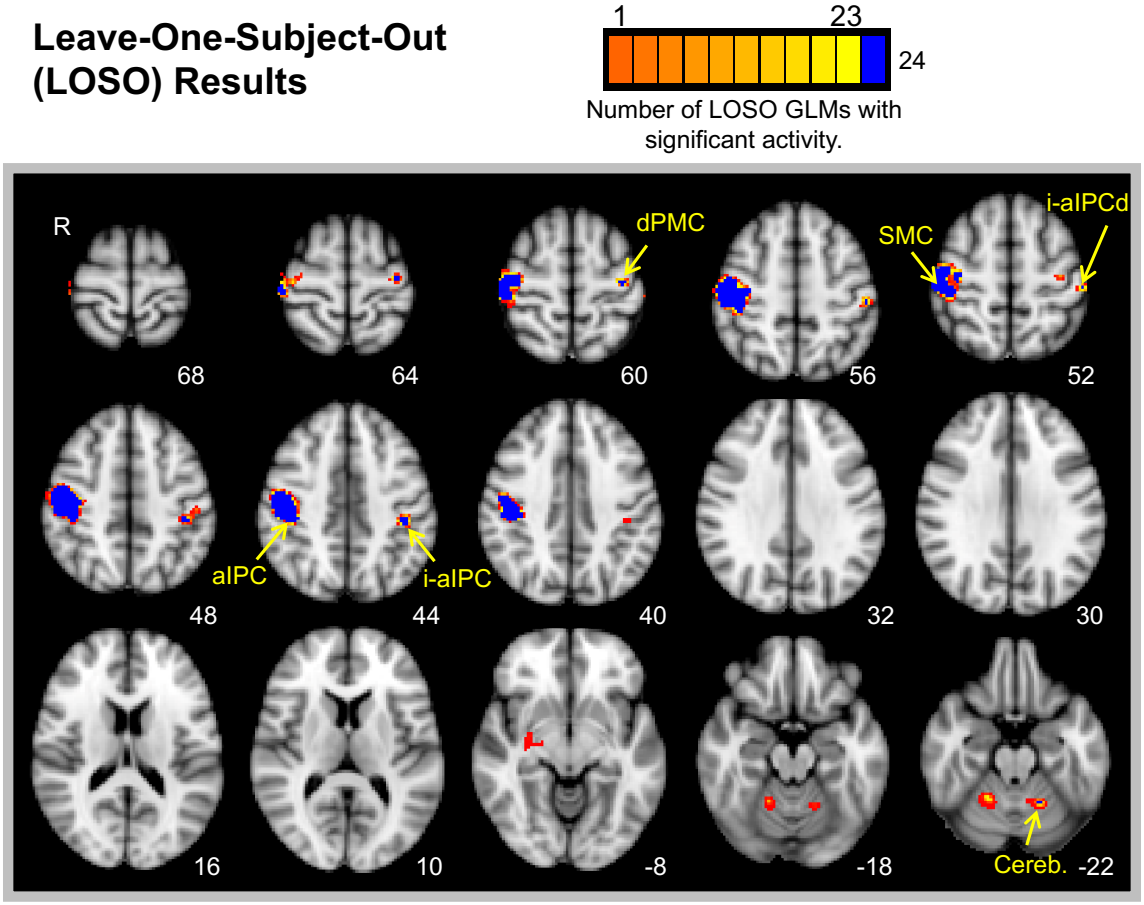


**Supplementary Figure 1. LOSO GLM overlap results.** Voxel-wise results showing the number of LOSO GLM results that identify significant activity for Grasp versus Touch. Blue coloured voxels indicate locations where all 24 LOSO GLM results reveal significant activity. These locations overlap with all six ROIs identified in Figure 4, based on the full group GLM. See Figure 4 for abbreviations.